

Article

The Effects of Particle Gradation on Salinized Soil in Arid and Cold Regions

Xuebang Huang ¹, Zizhao Zhang ^{1,2,*}, Ruihua Hao ¹ and Zezhou Guo ¹

¹ School of Geology and Mining Engineering, Xinjiang University, Urumqi 830046, China; hxb0714@163.com (X.H.); 18220186964@163.com (R.H.); xiangerji427@163.com (Z.G.)

² State Key Laboratory for Geomechanics and Deep Underground Engineering, Xinjiang University, Urumqi 830046, China

* Correspondence: zhangzizhao@xju.edu.cn; Tel.: +86-136-3997-7295

Abstract: Particle size grading impacts salt-frost heaving and dissolution collapse events of salinized soil on northwestern China's arid and cold region highways. However, the influencing mechanisms remain unclear and the impact of varying particle size grading needs further investigation. Hence, this study focused on these effects and the number of freeze–thaw cycles on the characteristic changes in highway salinized soil in arid and cold regions. Three soil columns with different gradations were prepared to explore the gradation and the number of freeze–thaw cycle affects on salinized soil's salt-frost heaving and dissolution collapse characteristics. The multi-functional physical simulation platform conducted multiple freeze–thaw cyclic tests in the laboratory. Test results confirmed significant and conclusive effects of gradation and the number of freeze–thaw cycles on salinized soil's salt-frost heaving and dissolution collapse behaviors. Poorly graded salinized soil with high coarse particle content caused repeated freeze and thaw engineering hazards, significantly affecting salinized soil's displacement and deformation behaviors during freezing. Contrarily, an increased range of fine particles more easily involved the characteristics of salinized soil during thawing. Therefore, the fourth freeze–thaw cycle was a crucial time node. After four freeze–thaw cycles, the displacement and deformation of original salinized soil and B-grade salinized soil samples (poorly graded with high fine particle content) tended to be stable. In contrast, the displacement and deformation of A-grade salinized soil samples (poorly graded with high coarse particle content) increased the growth rate. The present research results contribute to in-depth knowledge of the effects of gradation and freeze–thaw cycles on the characteristics of salinized soil in northwestern China, providing excellent referenced data support for the prevention and control of highway salinized soil failures and other engineering projects in arid and cold regions of northwest China.



Citation: Huang, X.; Zhang, Z.; Hao, R.; Guo, Z. The Effects of Particle Gradation on Salinized Soil in Arid and Cold Regions. *Water* **2022**, *14*, 236. <https://doi.org/10.3390/w14020236>

Academic Editor: Akbar Javadi

Received: 8 December 2021

Accepted: 11 January 2022

Published: 14 January 2022

Publisher's Note: MDPI stays neutral with regard to jurisdictional claims in published maps and institutional affiliations.



Copyright: © 2022 by the authors. Licensee MDPI, Basel, Switzerland. This article is an open access article distributed under the terms and conditions of the Creative Commons Attribution (CC BY) license (<https://creativecommons.org/licenses/by/4.0/>).

Keywords: particle gradation; freeze–thaw cycles; salinized soil; salt-frost heaving; dissolution collapse

1. Introduction

Saline soils are widely distributed in the world, and in China, saline soils are mainly distributed in the northwest of the country [1]. These areas are often located in seasonally frozen or permafrost regions. Salt-frost heave is caused by temperature changes and usually occurs in autumn, late winter or early spring [2,3]. The precipitation of salt crystals becomes very intense with the decrease of temperature [4]. Salinized soil extensively occurs in the Dushanzi Region (in the northern section of the Dushanzi–Kuqa Highway in Xinjiang). The salinized soil properties change with repeated temperature changes over many years, affecting the regular operation of engineering buildings [5–9]. For example, salt-frost heaving was the leading cause of the deformation and failure of highway subgrade. Dushanzi–Kuqa Highway, as a landscaped road passing through the ridge of Tianshan Mountain, is profoundly significant in connecting north and south Xinjiang, developing and constructing the frontier, shortening operating mileage, and facilitating

the economy. Previous studies have only poorly investigated the salinized soil distribution along the Dushanzi–Kuqa Highway. Hence, an in-depth exploration of salinized ground conditions on the Dushanzi–Kuqa Highway was strongly needed.

Scholars have conducted much single-factor research into salt-frost heaving behavior. Previous studies revealed that the salt expansion of sulfite soil dropped with the increasing content of sulfite under cyclic freeze–thaw conditions, and this development became more evident with higher sulfite content [10]. Meanwhile, the rising sulfite content contributed more significantly to the soil's variable expansion [11,12], while both heat conductivity and permeability coefficient dropped [13]. Hayley et al. obtained solute redistribution induced by moisture migration based on the variation of electrical conductivity in saline soils [14]. Most scholars agreed that salt-frost heaving increased with water content, which reached the maximum at an optimal water content and dropped after exceeding this point [15–17]. Some scholars agreed that both salt-frost heaving and dissolution collapse of salinized soil in freeze–thaw cycles occurred cumulatively [18–20]. After four freeze–thaw cycles, the soil-frost heaving cumulative speed of natural sulfite soil in Lop Nor began to drop [20]. The number of freeze–thaw cycles also imposed a particular effect on salt-frost heaving of the salinized soil. Pan Lei et al. found that the salt-frost heaving rate of Lop Nor natural salinized soil reached the maximum point at the fourth freeze–thaw cycle [21]; Na Shushu et al. concluded that the sulfate soil samples with different water contents of 10%, 13%, and 16% all reached the maximum salt-frost heaving increment at the third freeze–thaw cycle [22]. Ci Jun et al. found that sulfate soil samples with different water contents of 10% and 13% reached the maximum salt-frost heaving increment at the third freeze–thaw cycle, but sulfate soil with a water content of 16% reached the peak salt-frost heaving increment at the sixth freeze–thaw cycle [16]. The setting of different thawing temperatures may have resulted in the difference in test results. Other scholars indicated that the maximum cumulative salt-frost heaving was 3.14 mm after the seventh freeze–thaw cycle [21]. Undoubtedly, coarse particles decompose while fine particles aggregate under freeze–thaw action, increasing the pore diameter [23–26]; as the number of freeze–thaw cycles increased, salt-frost heaving increased at a decreasing rate [27]. Soil porosity dropped, and vertical permeability increased during freeze and thaw. Permeability increases the formation of polygonal contracted cracks and decreases fine-particle volume in pores among coarse particles [28].

The previous freeze–thaw cyclic tests revealed that the ionic solution property determined the soil's initial freezing temperature [29]. Additionally, the freezing point dropped with the increase in salinity but increased with increasing water content [30], which also fell with decrease of water activity, pore diameter, and unfrozen water content [31]. During the freezing process, salt crystals with layered distribution in the frozen zone formed the largest salt crystal distribution zone around the cool front under solute diffusion [32]. First, salt heaving occurred at 0 °C as the initial precipitation temperature of salt crystal; next, salt heaving and frost heaving appeared as the temperature fell [33,34].

Based on a single-factor investigation on salt-frost heaving of salinized soil, many scholars have focused on the multi-factor coupling effects on salt-frost heaving of salinized soil. Wen Tao et al. pointed out that salt-frost heaving salinized soil under freeze–thaw cycles resulted from volume change under salt and water phase-change action [35]. Younes [36] established a coupled model of water, heat and salt to predict concentration distribution in porous media, and established a coupled model of water and salt transport considering the influence of salt crystallization, but the influence of latent heat on temperature field was not considered [37]. Koniorczyk and Gawin [38] extended this by describing the effect of salt crystallization and dissolution on the conservation of salt mass.

Zhang Xudong et al. established the model for simulating the interaction among water, heat, and salt in salinized soil during the freezing process [39]. They also added the action of force in 2018 [40]. Zhang Shasha et al. revealed that salt, water, and temperature changes could be the main factors in salt expansion and deformation [13]. However, there was still a lack of systematic investigation of salt-frost heaving behavior of salinized soil

in the northwest of China, especially the effects of gradation of salinized soil on salt-frost heaving [41]. Wu Yaping et al. pointed out that the skeleton effect of coarse particles can inhibit the occurrence of dissolution collapse when the content of sodium sulfate remains unchanged. Still, the proportion of coarse particles increased, accompanied by weakened dissolution collapse [42].

In previous studies, scholars mainly selected water content, salinity, maximum dry density, the number of freeze–thaw cycles, and temperature. They conducted single-factor or multi-factor analysis to explore salt-frost heaving and dissolution collapse characteristics of salinized soil while neglecting the coupling effect of particle gradation and the number of freeze–thaw cycles on salt-frost heaving and dissolution collapse characteristics of salinized soil under an arid and cold climate in the northwest of China. Particle gradation affected highway construction, closely correlating with heaving and settlement of subgrade. Therefore, it was necessary to explore particle gradation's effect on subgrade and pavement under arid and cold climates. This study started with particle gradation and the number of freeze–thaw cycles on the salinized soil properties and conducted a large-size laboratory soil-column simulation test on salinized soil samples from Dushanzi–Kuqa Highway. The displacement and deformation rules of salinized soil samples with three different gradations, mainly salt-frost heaving amount/coefficient and dissolution collapse amount/coefficient, were analyzed to examine gradation relations and the number of freeze–thaw cycles along with highway salinized soil properties.

2. Materials and Methods

This section is organized as follows: (1) soil sampling and basic physical properties; (2) preparation of samples and test conditions.

2.1. Soil Sampling and Basic Physical Properties

In northwest China, most of the research areas targeted by scholars are in the ningxia saline soil research area, Xinjiang lop nur research area [16,19,21,22], Xinjiang aiding lake saline soil research area [15], and Xinjiang kashi saline soil research area [18,27]. The research results of duku highway saline soil research area in Xinjiang are relatively blank. Therefore, duku highway saline soil is the research object for the sampling work.

We used a 1.2 m long wooden-handle flat spade to collect natural salinized soil samples from the northern Dushanzi–Kuqa Highway (specifically, the alluvial-fluvial plain in the front of Dushanzi Mountain, the starting point of the Dushanzi–Kuqa Highway) at a sample interval of 0.5 m. We collected a total of 35 groups of the sample at a sampling depth of 0–30 cm. Each soil sample weighed approximately 10 kg, i.e., 350 kg salinized soil samples in total were collected. Figure 1 displays the exact positions of the sampling points.

First, the natural salinized soil samples collected from the Dushanzi–Kuqa Highway were separated into different sizes using an electric screen shaker. Then, after multiple repeated separations, soil samples were further sieved by a standard soil sieving device to ensure the obtaining of different size grouped soil samples for further preparation of soil columns.

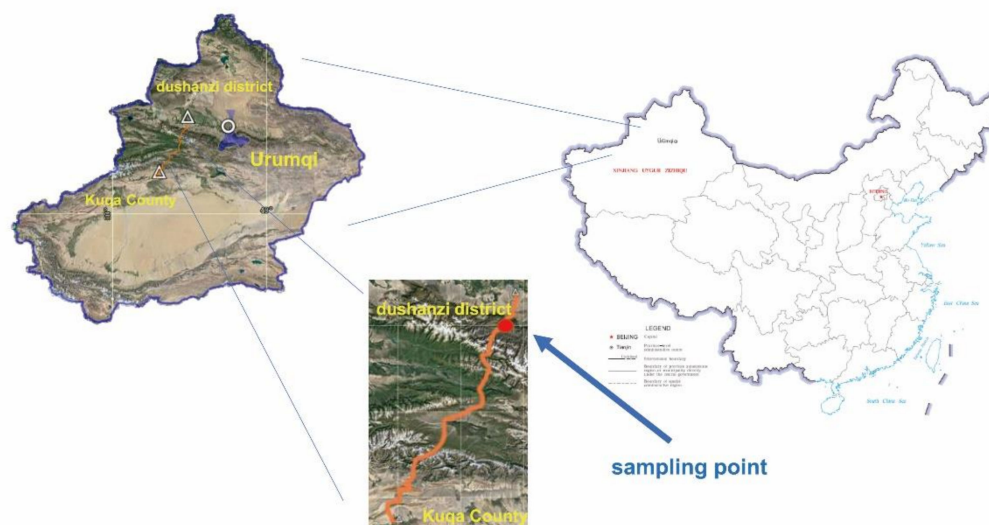


Figure 1. Location map of sampling point.

Previous research on the characteristics of saline soil seldom considered grading as a variable affecting the characteristics of saline soil [10–28,35–40], yet grading is a crucial factor for subgrade saline soil [43]. Therefore, this study focuses on grading as an influencing factor. By considering both advantages and disadvantages of the gradation of salinized soil, we prepared salinized soil samples with good gradation and poor gradation. Specifically, for good-gradation samples, $C_u > 5$ and $C_c = 1\sim 3$, where C_u and C_c denoted uniformity coefficient and curvature coefficient, respectively. The remaining were poorly graded. In this study, the salinized soil samples with original gradation were selected as the experimental group, while the samples with Gradation A and Gradation B (denoted as A-grade and B-grade soil samples) were the control group. As a result, A-grade samples were salinized soil with poor gradation and a high proportion of coarse particles, while B-grade samples were salinized soil with a high proportion of fine particles. In addition, the above gradations were set for exploration of the effects of gradation quality and particle size on the characteristics of salinized soil, thereby providing specific guidance for actual engineering.

For original salinized soil samples, the proportion of fine particles with a diameter of below 0.075 mm was 50.15%, and the particle sizes were mainly distributed within a range of 0.075~0.25 mm; additionally, $C_u = 23.33$ and $C_c = 1.71$, suggesting well-graded fine-grained soil. For A-grade salinized soil samples, the proportion of fine particles with a diameter of below 0.075 mm was only 2.88%, and the particle sizes were mainly distributed within a range of 1~2 mm; additionally, $C_u = 2.5$ and $C_c = 3.13$, suggesting poorly graded coarse-grained soil. For B-grade salinized soil samples, the proportion of fine particles with a diameter of below 0.075 mm was only 43.23%, and the particle sizes were mainly distributed within a range of 0.075~0.25 mm; additionally, $C_u = 75$ and $C_c = 50.02$, suggesting poorly-graded fine-grained soil. Table 1 lists the fundamental physical properties of these salinized soil samples. Table 2 lists the proportions of the particles with different sizes in three different salinized soil samples with different gradations, and Figure 2 shows the particle size distribution patterns for three different types of salinized soil sample.

Table 1. List of basic physical property parameters of saline soil.

Basic Physical Property Parameters	Numerical Value
Liquid limit, W_p (%)	25.4
Plastic limit, W_L (%)	10.1
Plastic index, I_p	15.36
Liquidity index, I_L	−0.61
Optimal moisture content, w_{opd} (%)	3.88
Maximum dry density, $\rho_{d,max}$ (g/cm ³)	1.897
Coefficient of uniformity, $C_u = d_{60}/d_{10}$	13.07

Table 2. Percentage table of sample particle size distribution.

Type	Parameters	Numerical Value					
The original grade	grain size (mm)	5–20	2–5	1–2	0.5–1	0.25–0.5	0.075–0.25
	proportion (%)	4.91	5.72	3.21	16.35	0	19.66
	grain size (mm)	0.057–0.075	0.028–0.057	0.012–0.028	0.006–0.012	0.005–0.006	<0.005
	proportion (%)	10.47	15.71	9.09	4.63	0.33	9.92
A-grade	grain size (mm)	5–20	2–5	1–2	0.5–1	0.25–0.5	0.075–0.25
	proportion (%)	14.12	25.36	30.26	15.85	0	11.53
	grain size (mm)	<0.075					
	proportion (%)	2.88					
B-grade	grain size (mm)	5–20	2–5	1–2	0.5–1	0.25–0.5	0.075–0.25
	proportion (%)	14.12	6.48	12.39	8.21	0	15.56
	grain size (mm)	0.057–0.075	0.028–0.057	0.012–0.028	0.006–0.012	0.005–0.006	<0.005
	proportion (%)	9.03	13.54	7.84	3.99	0.29	8.55

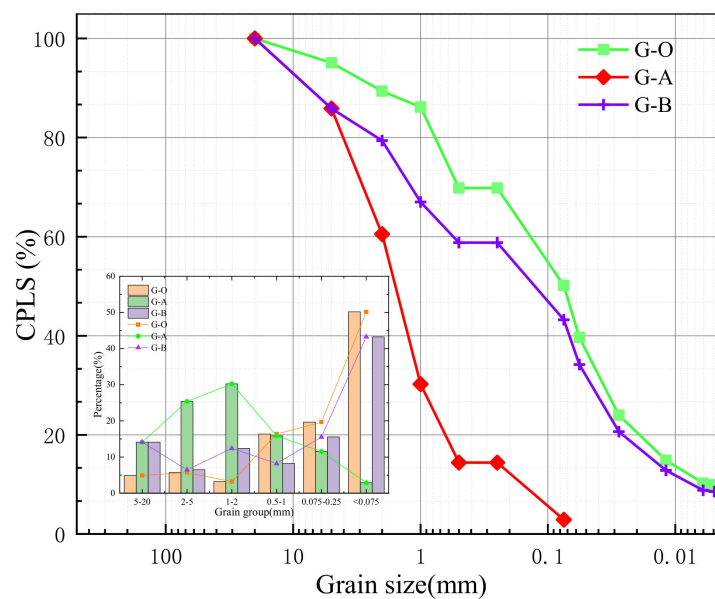


Figure 2. Grain size distribution of the soil sample (Note: CPLS is cumulative percentage less than certain particle size; G-O denotes the original grading; G-A denotes A grading; G-B denotes B grading).

2.2. Preparation of Samples and Test Conditions

This section is organized as follows: (1) a brief introduction of the natural condition; (2) preparation of samples; (3) test condition.

2.2.1. A Brief Introduction of the Natural Condition

Dushanzi, located at the northern foot of the Tianshan Mountain and the southwestern edge of Junggar Basin, is contiguous to the Tianshan Mountains (as the southern barrier) and borders Kuitun City and the National Highway 312, with Wusu City to the west, and Shawan County to the east. We analyzed atmospheric temperature data over consecutive years from 2011 to 2020 from Dushanzi Meteorological Station, to conclude that summer in Dushanzi lasted from June to August, with a mean temperature of 20–30 °C and an extremely high temperature of 34 °C, and winter lasted from December to February during the next year, with a mean temperature of −10~−18 °C and a low temperature of −27 °C. The temperature fluctuated significantly in winter.

2.2.2. Preparation of Samples

According to the Technical Standard of Highway Engineering [44], the compaction degree of soil sample was 93%, i.e., the dry density of soil after the compaction in the Acrylic soil column instrument was 93% of the maximum dry density, and the moisture content was the same as the optimal moisture content of the soil sample (3.88%). Therefore, the mass control method kept the dry density of the sample at 1.897 g/cm³. The prepared soil samples were placed in sealed preservation bags for 24 h, so samples became fully moisturized. On the next day, the soil samples were divided into six layers and compacted into the soil column instrument with a size of 90 mm × 300 mm layer by layer, during which the molding temperature was 20 °C.

2.2.3. Test Condition

As described above, we prepared the soil samples with three different gradations (original gradation, B-grade, and A-grade) for laboratory large-size soil-column simulation tests under different freeze–thaw cycles. For extreme weather simulation, we set the freezing and thawing temperatures as −30 °C and 35 °C during the freeze and thaw time of 12 h. Therefore, each group of soil samples underwent seven different freeze–thaw cycles with varying numbers of freeze–thaw cycles. Thus, this study established the maximum and minimum freeze–thaw processes as 7 and 1, respectively.

As shown in Figure 3a, a freezing–thawing cycle and automatic monitoring system was set up in this test, which is different from the test equipment used in previous studies. The freezing–thawing cycle and automatic monitoring system mainly consisted of the soil-column instrument, the multi-functional physical simulation test platform, the data acquisition system, the DataTakerDT85G data acquisition instrument, the temperature sensor, Delogger data acquisition software, the displacement sensor, and the computer.

The influence of initial temperature was eliminated in the soil columns after compaction by equilibration on the multi-functional physical simulation test platform at a fixed temperature of 5 °C. Moreover, the initial temperature was accurately checked and set for constant-temperature preservation for 8 h. After temperature equilibrium was complete, formal freeze–thaw tests commenced. The multi-functional physical simulation test platform reached the freezing temperature of −30 °C within half an hour. It maintained the freezing temperature for 11.5 h, then reached the thawing temperature of 35 °C within half an hour and held the thawing temperature for 11.5 h, i.e., a complete freeze–thaw cycle lasted 24 h. Figure 4 displays the variation curves of temperature with time. Since No. 1 and No. 2 temperature sensors were far away from the outlet of the box (especially, No. 1 sensor was further away from the outlet), the values of the measured temperature by these two sensors were lower than actually designed freezing and thawing temperatures. As shown in Figure 3b, the soil column instrument was coated with a layer of insulating cotton to prevent heat exchange between the sample and the surrounding environment.



Figure 3. Test site layout: (a) Multifunctional physical simulation test platform (b) Soil column ready for test.

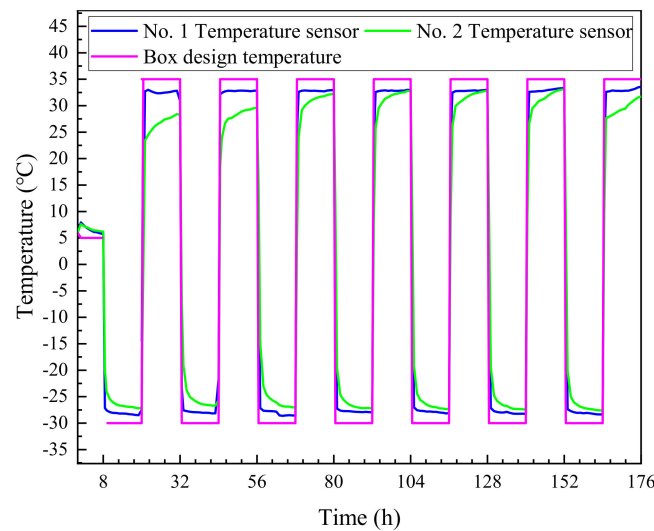


Figure 4. Box temperature during freeze–thaw cycle.

The constantan thermocouples, with a temperature range of $-50\sim 50\text{ }^{\circ}\text{C}$, were adopted as temperature sensors. The temperature probe was comprised of copper and constantan. The sensor was cemented with AB glue to ensure sealing and water resistance. The D050-type sensor procured the detailed parameters in Table 3. Automatic compensation eliminated any temperature effects. Before the test, we calibrated the temperature sensor and the displacement sensor, as shown in Figure 5. Figure 6 displays the flowchart for the large-size soil-column freeze–thaw test.

Table 3. Parameters of displacement sensor.

Product Model	Range	Measurement Accuracy	Mode of Connection	Temperature Range
D050	50 mm	0.01 mm	half-bridge	$-35\text{ }^{\circ}\text{C}\sim 70\text{ }^{\circ}\text{C}$



Figure 5. Sensor calibration: (a) Calibration of displacement sensor with screw micrometer (b) Temperature sensor calibration.

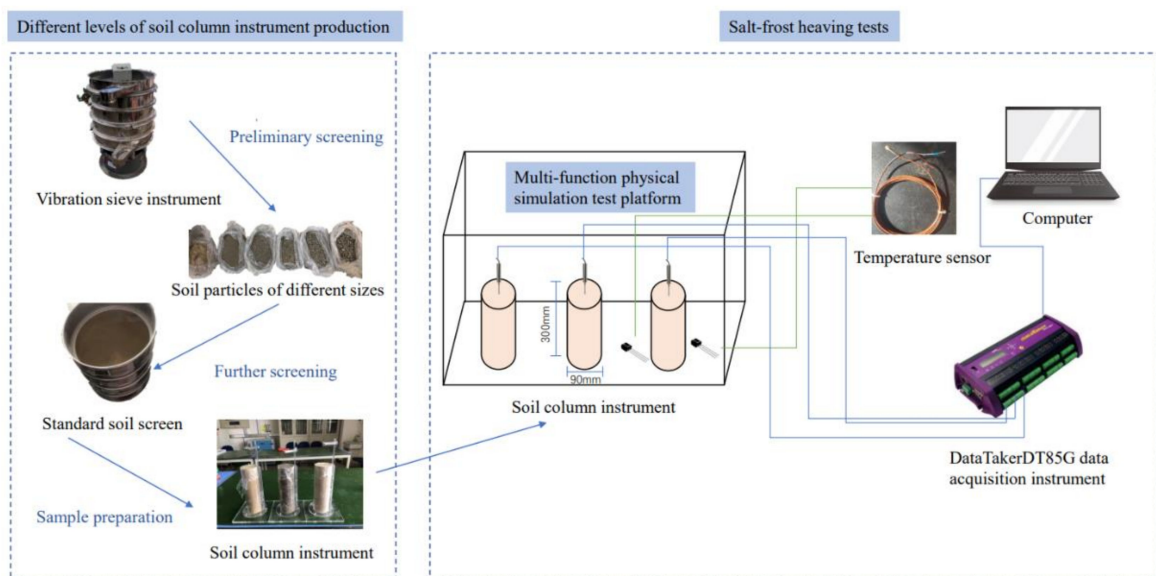


Figure 6. Flow chart of freeze-thaw cycle test of large soil column.

3. Results and Analysis

This section is organized as follows: (1) displacement and deformation rules of the salinized soil samples with different gradations; (2) dissolution collapse and salt-frost heaving behaviors of salinized soil samples with different gradations; (3) freeze–thaw duration curves of the prepared salinized soil samples with different gradations.

3.1. Displacement and Deformation Rules of the Salinized Soil Samples with Different Gradations

By performing a laboratory large-size soil-column simulation test, we examined the displacement and deformation rules of the prepared salinized soil samples with the three different test gradations under other freeze–thaw cyclic conditions, and the results are seen in Figure 7.

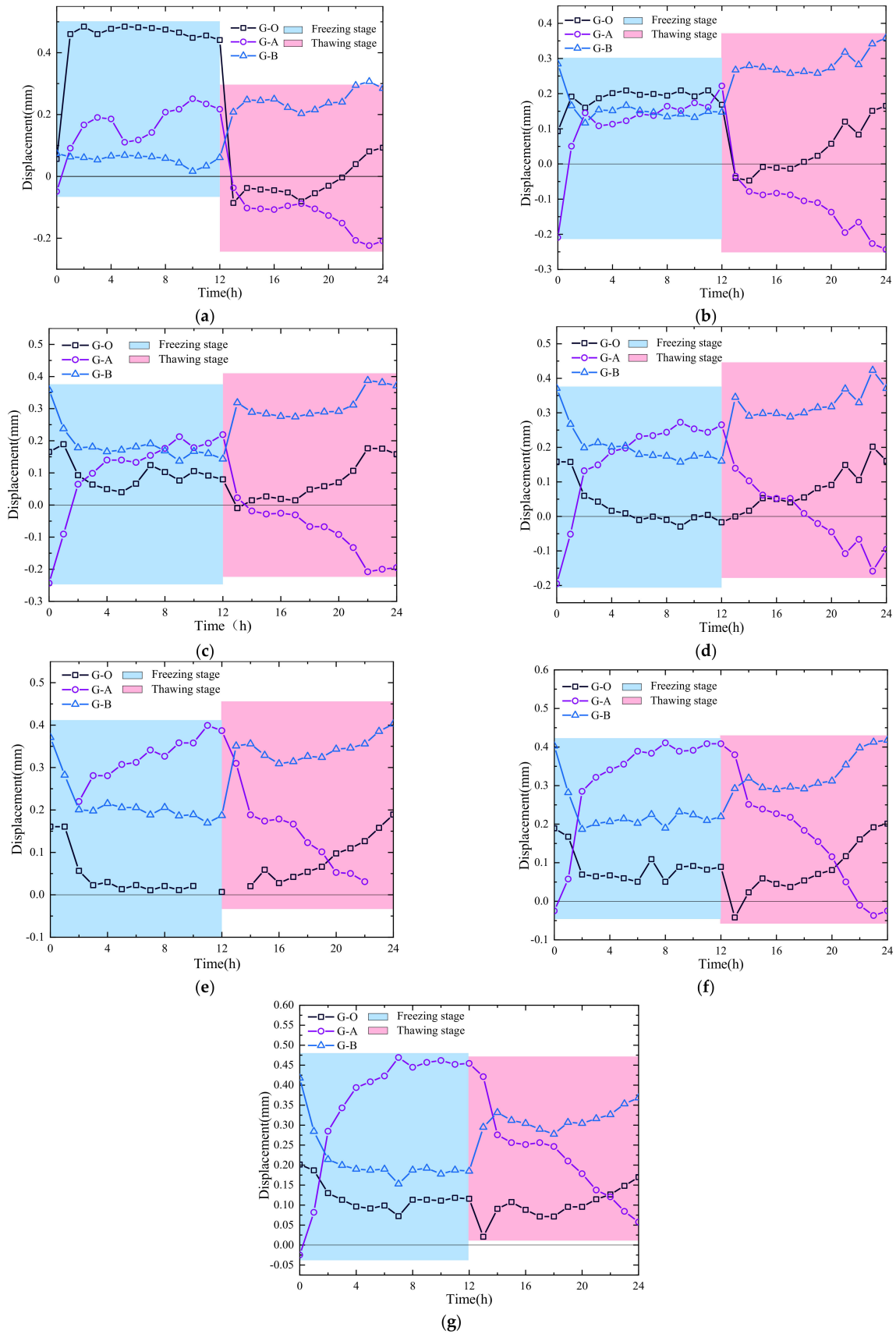


Figure 7. Displacement deformation under different freeze–thaw cycles: (a) freeze–thaw cycle once (b) freeze–thaw cycles two times (c) freeze–thaw cycles three times (d) freeze–thaw cycles four times (e) freeze–thaw cycles five times (f) freeze–thaw cycles six times (g) freeze–thaw cycles seven times.

Overall, different salinized soil samples with three different gradations show different variation rules after the same freeze–thaw cycles, and the samples with the same gradation show different variation rules after different freeze–thaw cycles.

(1) Variation rules at the thawing phase

In the first seven freeze–thaw cycles, the displacement and deformation of the A-grade salinized soil samples at the thawing phase were lower than those at the freezing stage. In contrast, the B-grade salinized soil samples showed opposite rules at different phases (i.e., the displacement and deformation at the thawing phase were higher than those at the freezing stage), and the salinized soil samples with original gradation lay between the above two variation rules. Since the salinized soil with poor gradation had a more significant porosity and permeability coefficient, the specific surface areas of water molecules in the pores were more effective. As the proportion of coarse particles increases, both porosity and permeability coefficient increase, and water content is more easily increased, thereby increasing both salt heaving and frost heaving. Accordingly, from a macroscopic perspective, the displacement and deformation of the salinized soil samples with A-grade at the freezing stage exceeded those at the thawing stage.

On the other hand, the samples with B-grade showed opposite patterns, displacement and deformation at the thawing stage exceeding those at the freezing stage, which is mainly attributed to the high content of fine particles in the salinized soil with B-grade, thereby resulting in the enhanced activity of soil particles. As a result, the soil expands with rising temperature at the thawing stage, and therefore soil expansion at the thawing phase exceeded salt-frost heaving at the previous freezing phase. In addition, we observed that the salinized soil samples with different gradations showed similar variation rules after different freeze–thaw cycles. For example, the salinized soil samples with three gradations showed similar displacement and deformation rules after two and three freeze–thaw cycles; for the three types of the salinized soil sample, the various rules of displacement and deformation were also similar after five and seven cycles.

At the thawing phase, the displacement and deformation of these three types of samples showed a more significant difference. Specifically, the displacement and deformation of B-grade salinized soil exceeded those of original and A-grade salinized soil. The intersection point existed between original and A-grade salinized soil samples (i.e., the lead changed between A-grade and actual soil samples after the intersection point). As the number of freeze–thaw cycles increased, and the intersection point appeared later, from initially 12 to finally 22 h. This suggested that the previous displacement and deformation of A-grade salinized soil increased with the number of freeze–thaw cycles more rapidly than that of the original salinized soil at the thawing phase.

(2) Variation at the thawing phase

At the freezing phase, the displacement and deformation curves of the three types of salinized soil samples overlapped in the second and third freeze–thaw cycles but were scattered in the others. Notably, the curves were most dispersed in the seventh freeze–thaw cycle, suggesting apparent differentiation after seven freeze–thaw cycles. After a freeze–thaw process, the displacement and deformation of the salinized soil samples with original gradation reached the maximum, dropping gradually since the second cycle. The displacement and deformation of the original soil sample were lower than those of A-grade and B-grade samples after the second freeze–thaw cycle. The intersection point between A-grade and B-grade samples' displacement and deformation curves began to move forward since the third freeze–thaw cycle, which moved from the original 8 h forward to 14 h. After the intersection, the displacement and deformation of A-grade salinized soil samples far exceeded that of B-grade samples.

Conclusively, the increasing content of coarse particles in the soil contributed to the displacement and deformation of soil at the freezing phase, while the increased fine particles content affected the soil displacement and deformation at the thawing stage. Therefore, poor gradation influenced soil displacement and deformation over the freeze–thaw cycle.

3.2. Dissolution Collapse and Salt-Frost Heaving Behaviors of Salinized Soil Samples with Different Gradations

Next, the various rules of salt-frost heaving amount and coefficient, dissolution collapse amount and coefficient different salinized soil samples with three different gradations were investigated in-depth via a laboratory large-size soil-column simulation test, shown in Figures 8 and 9.

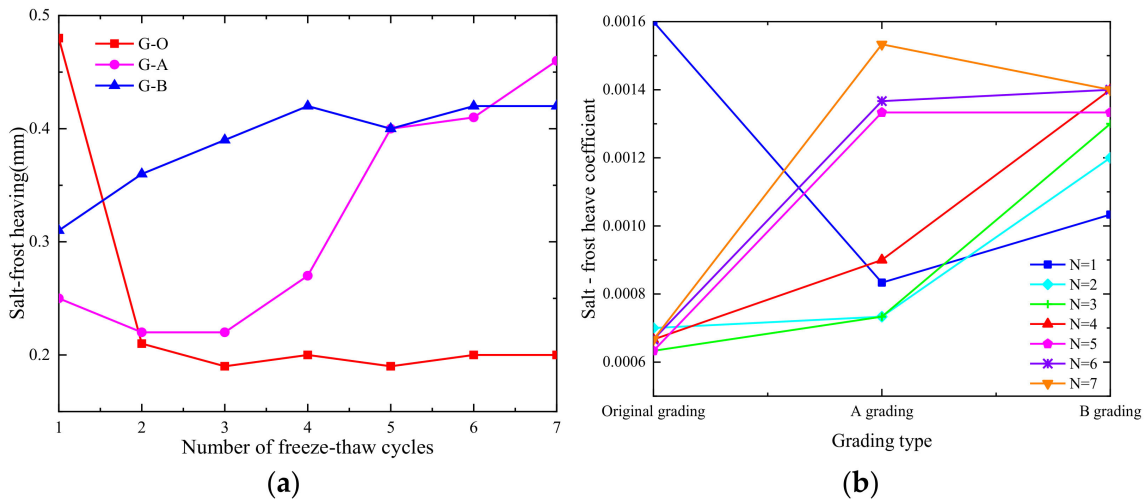


Figure 8. Salt-frost heaving and salt-frost heaving coefficient of saline soil with different gradation: (a) Salt-frost heaving (b) Salt-frost heave coefficient.

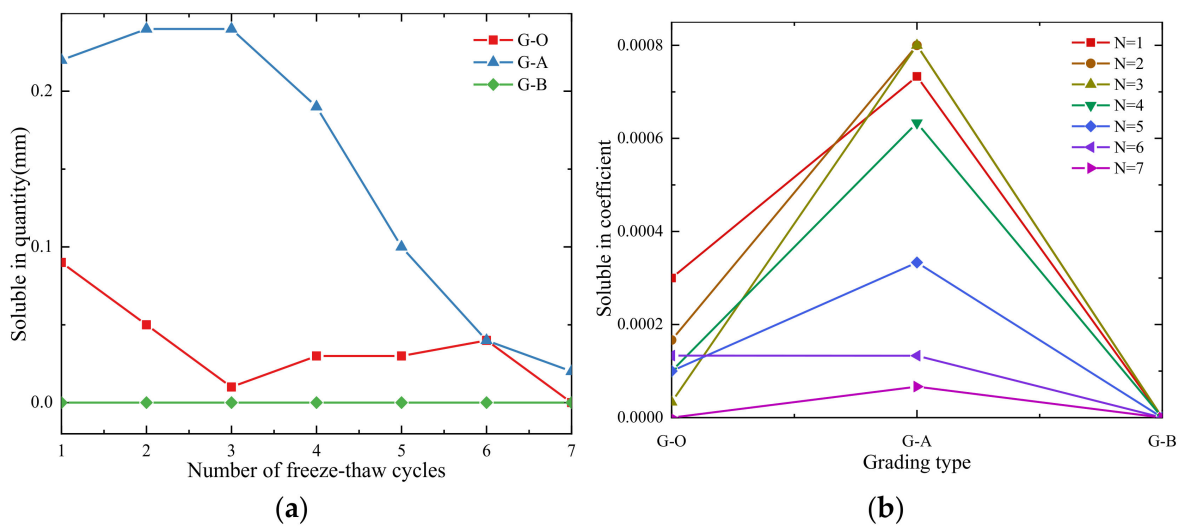


Figure 9. The amount and coefficient of settlement of saline soil at different levels: (a) Soluble in quantity (b) Soluble in coefficient.

3.2.1. Salt-Frost Heaving Amount and Salt-Frost Heaving Coefficient

The measured statistical parameters from the results listed in Table 4 explored the variation rules for salt-frost heaving parameters of salinized soil samples after different freeze-thaw cycles. Figure 8 shows the salt-frost heaving behaviors of different soil samples after multiple freeze-thaw cycles and the related correlation coefficients.

Table 4. Statistical table of dissolution and salt-frost heave of samples.

Number of Freeze-Thaw Cycles	The Original Grading		A-Grade		B-Grade	
	Salt-Frost Heaving Amount (mm)	Salt-Frost Heaving Coefficient	Salt-Frost Heaving Amount (mm)	Salt-Frost Heaving Coefficient	Salt-Frost Heaving Amount (mm)	Salt-Frost Heaving Coefficient
1	0.48	0.001600	0.25	0.000833	0.31	0.001033
2	0.21	0.000700	0.22	0.000733	0.36	0.001200
3	0.19	0.000633	0.22	0.000733	0.39	0.001300
4	0.2	0.000667	0.27	0.000900	0.42	0.001400
5	0.19	0.000633	0.4	0.001333	0.4	0.001333
6	0.2	0.000667	0.41	0.001367	0.42	0.001400
7	0.2	0.000667	0.46	0.001533	0.42	0.001400

Combining Table 4 and Figure 8 helped conclude that both salt-frost heaving amount and coefficient of original salinized soil sample first dropped and then tended to be stable along with the increasing number of freeze–thaw cycles, while the salt-frost heaving parameters of A-grade and B-grade salinized soil samples increased steadily. Further, the salt-frost heaving amount and coefficient of A-grade soil increased at a more significant velocity. Overall, the salt-heaving amount of B-grade soil was most significant and reached a maximum of 0.48 mm, followed by the value for A-grade soil with a maximum of 0.46 mm, and finally, the value of original salinized soil, with a maximum of 0.42 mm. After six freeze–thaw cycles, the salt-frost heaving of A-grade salinized soil exceeded that of B-grade soil. After the first four freeze–thaw cycles, the salt-frost heaving coefficients of B-grade salinized soil exceeded those of A-grade and original soil samples, and the salt-frost heaving coefficients of A-grade salinized soil. The rest of the three freeze–thaw cycles exceeded those of B-grade and original soil samples. Results indicated that poor gradation contributed to the increasing salt-frost heaving amount of salinized soil, and good gradation inhibited this. Under poor gradation, too significant proportions of fine and coarse particles promoted the increase of salt-frost heaving; to be specific, fine particles imposed a more substantial effect on the promotion of heaving over a short time while coarse particles played a more remarkable role in the long term. For soil with good gradation, both porosity and permeability coefficient were lower, and therefore, the specific surface area for filling water in pores was smaller, suggesting a slight increase of water content. For poorly-graded soil, both porosity and permeability coefficient were more significant, and therefore the specific surface area for filling water in pores was greater. In the short run, many fine particles can increase the specific surface area of poor-gradation salinized soil, leading to the rapid increase of salt-frost heaving amount and coefficient at the macro-level. Many coarse particles can increase the spacing among particles in the long run. Meanwhile, large particles in the soil can be decomposed into small particles under freeze–thaw cyclic action, increasing water content and subsequent salt-frost heaving. Cumulatively, both salt-frost heaving amount and coefficient of A-grade salinized soil reached the maxima late.

3.2.2. Dissolution Collapse Amount and Dissolution Collapse Coefficient

The dissolution collapse amount and the statistics of its coefficient were explored to find the varied rules of dissolution collapse parameters after different freeze–thaw cycles, as listed in Table 5. Figure 9 shows the dissolution collapse behaviors of varying soil samples after multiple freeze–thaw cycles and the related correlation coefficients.

Table 5. The amount and coefficient of dissolution of soil samples.

Number of Freeze-Thaw Cycles	The Original Grading		A-Grade		B-Grade	
	Dissolution Collapse Amount (mm)	Dissolution Collapse Coefficient	Dissolution Collapse Amount (mm)	Dissolution Collapse Coefficient	Dissolution Collapse Amount (mm)	Dissolution Collapse Coefficient
1	0.09	0.000300	0.22	0.000733	0	0
2	0.05	0.000167	0.24	0.000800	0	0
3	0.01	0.000033	0.24	0.000800	0	0
4	0.03	0.000100	0.19	0.000633	0	0
5	0.03	0.000100	0.10	0.000333	0	0
6	0.04	0.000133	0.04	0.000133	0	0
7	0	0	0.02	0.000067	0	0

The following observations are from Table 5 and Figure 9. For original salinized soil, both dissolution collapse amount and coefficient first dropped. After that, they tended to be stable and finally settled with the increasing number of freeze–thaw cycles, and fell to 0 after seven cycles. For A-grade salinized soil, both dissolution collapse amount and coefficient varied slightly in the first three freeze–thaw cycles (within a range of 0.22~0.24 mm and 0.0007~0.0008, respectively) and decreased drastically after the fourth cycle at a more significant decreasing rate than that of the original salinized soil. For B-grade salinized soil, no dissolution collapse was apparent. Overall, the dissolution collapse amount of A-grade salinized was significant, with a maximum of 0.24 mm, followed by original salinized soil, with a maximum of 0.09 mm, and finally, no dissolution collapse occurred in B-grade salinized soil. After the same number of freeze–thaw cycles, no dissolution collapse appeared with the increasing proportion of fine particles, suggesting that the formation of a fine-particle skeleton inhibited the occurrence of soil collapse. As the proportion of coarse particles increased, both dissolution collapse amount and coefficient reached the maxima, indicating dissolution collapse in soil. However, as the number of freeze–thaw cycles indicating that the formation of coarse-particle skeleton promoted the occurrence increased, and both dissolution collapse amount and coefficient of A-grade and original salinized soil samples dropped, which confirmed the inhibition of dissolution collapse by freeze–thaw cycles.

Moreover, the inhibition was cumulative to a certain degree. After freeze–thaw cycles, both salt-frost heaving and coefficient increased, which inhibited both Karst depression amount and coefficient of salinized soil. Some scholars [43,44] found that the equivalent pore diameter dropped along with the decrease of particle size, accompanied by an increasing number of pores and the deterioration of permeability; accordingly, the air or water intake values increased, water hardly discharged, and matrix suction increased. The spacing among particles in soil was filled by water or air with specific support, and therefore almost no or only slight collapse occurred. Otherwise, as the proportion of coarse particles increased and the ratio of fine particles dropped, the equivalent diameter of pores increased, the number of pores dropped, permeability enhanced, matrix suction dropped, both water and air quickly discharged, and at macro-level both dissolution collapse amount and coefficient increased.

3.3. Freeze–Thaw Duration Curves of the Prepared Salinized Soil Samples with Different Gradations

Finally, the displacement and deformation duration curves of the salinized soil samples with different gradations under freeze–thaw cyclic action were plotted by combining the results during seven freeze–thaw cycles, and the prediction in the following cycles are seen in Figure 10.

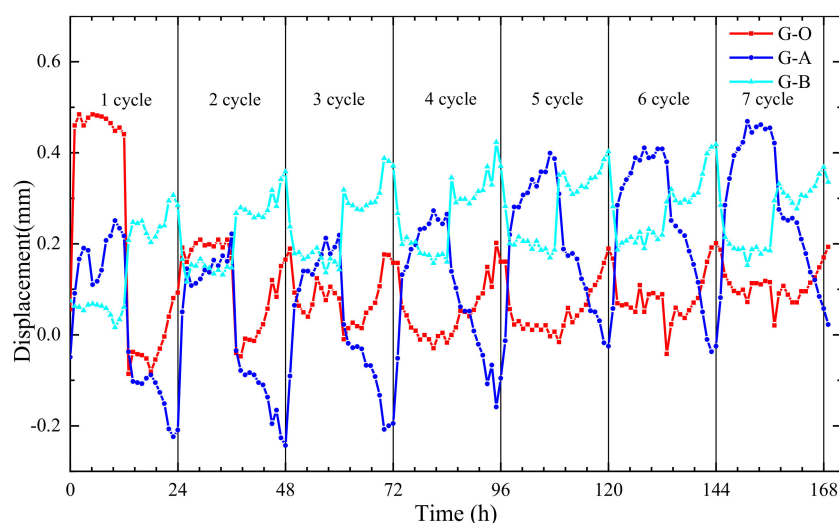


Figure 10. Process and duration curve of salt-frost heave of saline soil at different levels.

With increased freeze–thaw cycles, the displacement and deformation of original salinized soil first increased, then dropped, and finally stabilized after the fourth freeze–thaw cycle. The displacement and deformation of A-grade salinized soil increased steadily, with further increasing rate after the fourth freeze–thaw cycle. The displacement and deformation of B-grade salinized soil first increased and then became stable at the fourth freeze–thaw cycle. For original salinized soil, the displacement and deformation curve in the first freeze–thaw cycle showed a noticeable difference from the curves in the subsequent six cycles. As the number of freeze–thaw cycles increased, the effects of temperature on displacement and deformation curves of original salinized soil became more similar; after the sixth cycle, the original salinized soil reached a new equilibrium. The displacement and deformation variation curve showed an obvious w-shaped pattern for original salinized soil with time. For A-grade salinized soil, the deformation and displacement increased significantly after the fourth freeze–thaw cycle, and the variation curve became a downward-parabola pattern with the increasing number of freeze–thaw cycles. For B-grade salinized soil, the variation curve of displacement and deformation with time became a w-shaped pattern with increasing cycles. Conclusively, the displacement and deformation of A-grade salinized soil increased steadily with the number of freeze–thaw cycles, which then exceeded those of original and B-grade salinized soil samples. The displacement and deformation of B-grade salinized soil exceeded the original soil samples.

4. Conclusions

Some test parameters, including the number of freeze–thaw cycles, environmental temperature, and particle grading, were selected for analysis of the variation rules of overall displacement and deformation, and salt-frost heaving amount and coefficient, dissolution collapse amount and coefficient of different salinized soil samples with varying gradations under other freeze–thaw cyclic condition were investigated in depth. The main conclusions are as follows.

1. For the same number of freeze–thaw cycles, no dissolution collapse occurred in B-grade salinized soil, suggesting the inhibition of soil collapse by the formation of a fine-particle skeleton. On the other hand, both dissolution collapse amount and coefficient increased steadily in A-grade soil because of its large proportion of coarse particles, which indicated that the formation of a coarse particle structure promoted dissolution collapse in salinized soil.
2. When the number of freeze–thaw cycles remained unchanged, the increased proportion of fine or coarse particles promoted salt-frost heaving of salinized soil to a certain

- degree. Fine particles initially played a more significant role, but coarse particles made a more outstanding contribution in the long run.
3. Three types of salinized soil with different gradations showed similar variation rules of displacement and deformation after the second and the third freeze–thaw cycles. In addition, similar variation rules were observed for displacement and deformation after the fifth and the seventh freeze–thaw cycles. The displacement and deformation of original and B-grade salinized soil samples tended to be stable after the fourth freeze–thaw cycle, while A-grade soil showed rapidly increasing deformation and displacement after the fourth cycle. However, after seven freeze–thaw cycles, the displacement and deformation differed significantly among the three types of salinized soil sample.
 4. As the number of freeze–thaw cycles increased, the displacement and deformation of poor-gradation salinized soil with a high proportion of coarse particles changed significantly in the freezing phase. In contrast, the displacement and deformation of poor-gradation salinized soil with a high proportion of fine particles changed substantially in the thawing phase. Freeze–thaw cycles promoted both salt-frost heaving amount and coefficient of salinized soil and simultaneously inhibited both dissolution collapse amount and coefficient. Both promotion and inhibition were cumulative in the long-term freeze–thaw cyclic process. Therefore, in salinized soil with poor gradation, exceptionally high proportion of coarse particles can pose hazards to engineering, and the corresponding precautionary measures need to be available in advance.
 5. It should be noted that this experimental work is only applicable to saline soil. Further studies should investigate related geomaterials.

Author Contributions: Conceptualization, X.H.; methodology, X.H.; validation, X.H., Z.G. and R.H.; formal analysis, Z.Z.; investigation, Z.G. and R.H.; resources, X.H.; data curation, X.H.; writing original draft preparation, X.H.; writing-review and editing, X.H.; visualization, Z.Z.; supervision, X.H.; project administration, Z.Z.; funding acquisition, Z.Z. All authors have read and agreed to the published version of the manuscript.

Funding: This research was funded by the Open Foundation of State Key Laboratory for Geomechanics and Deep Underground Engineering (SKLDUEK2028) and the Special Program for Key Research and Development Tasks of Xinjiang Uygur Autonomous Region (2021B03004).

Institutional Review Board Statement: Not applicable.

Informed Consent Statement: Not applicable.

Data Availability Statement: The data used to support the findings of this study are included within the manuscript.

Conflicts of Interest: The authors declare that there are no conflict of interest.

References

1. Szabolcs, I. Amelioration of soils in salt affected areas. *J. Soil Technol.* **1989**, *2*, 331–344. [[CrossRef](#)]
2. Padilla, F.; Villeneuve, J.P. Modeling and experimental studies of frost heave including solute effects. *J. Cold Reg. Sci. Technol.* **1992**, *20*, 183–194. [[CrossRef](#)]
3. Blaser, H.D.; Scherer, O.J. Expansion of soils containing sodium sulfate caused by drop in ambient temperatures. *J. Highw. Res. Board Spec. Rep.* **1969**, *103*, 150–160.
4. Benavente, D.; Sanchez-Moral, S.; Fernandez-Cortes, A.; Cañaveras, J.C.; Elez, J.; Sáiz-Jiménez, C. Salt damage and microclimate in the Postumus Tomb, Roman Necropolis of Carmona, Spain. *J. Environ. Earth Sci.* **2011**, *63*, 1529–1543. [[CrossRef](#)]
5. Nixon, J.F. Discrete ice lens theory for frost heave beneath pipelines. *J. Can. Geotech. J.* **1992**, *29*, 487–497. [[CrossRef](#)]
6. Koniorczyk, M. Salt transport and crystallization in non-isothermal, partially saturated porous materials considering ions interaction model. *J. Int. J. Heat Mass Transf.* **2012**, *55*, 665–679. [[CrossRef](#)]
7. Naillon, A.; Joseph, P.; Prat, M. Ion Transport and Precipitation Kinetics as Key Aspects of Stress Generation on Pore Walls Induced by Salt Crystallization. *J. Phys. Rev. Lett.* **2018**, *120*, 034502. [[CrossRef](#)]
8. Melnikov, A.E.; Grib, N.N. Influence of frost weathering on the recession of surfaces of technogenic landforms in Yakutia. *J. Sci. Cold Arid. Reg.* **2019**, *11*, 257–266.

9. Choo, J.; Sun, W. Cracking and damage from crystallization in pores: Coupled chemo-hydro-mechanics and phase-field modeling. *J. Comput. Methods Appl. Mech. Eng.* **2018**, *335*, 347–379. [[CrossRef](#)]
10. Yang, Q.S.; Wu, Y.P.; Yu, T.Y. Experimental Study on Salt Expansion Characteristics of Sulfurous Saline Soil for Tehran-Isfahan High Speed Railway in Iran. *J. Railw. Eng.* **2019**, *59*, 96–99. (In Chinese)
11. Tang, R.; Zhou, G.Q.; Wang, J.Z.; Zhao, G.; Lai, Z.; Jiu, F. A new method for estimating salt expansion in saturated saline soils during cooling based on electrical conductivity. *J. Cold Reg. Sci. Technol.* **2020**, *170*, 102943. [[CrossRef](#)]
12. Zhang, J.; Lai, Y.M.; Zhao, Y.H.; Li, S. Study on the mechanism of crystallization deformation of sulfate saline soil during the unidirectional freezing process. *J. Permafrost. Periglac. Processes* **2020**, *32*, 102–118. [[CrossRef](#)]
13. Zhang, S.S.; Zhang, J.S.; Gui, Y.L.; Chen, W.; Dai, Z. Deformation properties of coarse-grained sulfate saline soil under the freeze-thaw-precipitation cycle. *J. Cold Reg. Sci. Technol.* **2020**, *177*, 103121. [[CrossRef](#)]
14. Hayley, K.; Bentley, L.R.; Gharibi, M. Time-lapse electrical resistivity monitoring of salt-affected soil and groundwater. *J. Water Resour. Res.* **2009**, *45*, W07425. [[CrossRef](#)]
15. Ye, M.; Pan, L.; Zhang, Y.F. Experimental Study on Salt-Frost Heave Characteristics of Natural Sulfite Saline Soil under the Effects of Multi-factors. *J. Henan Sci.* **2019**, *37*, 1276–1282. (In Chinese)
16. Ci, J.; Zhang, Y.F.; Na, S.S. Law of salt expansion of Lop Nur's nature saline soil under condition of freeze-thaw cycle. *J. Water Resour. Water Eng.* **2016**, *27*, 194–197. (In Chinese)
17. Dong, X.M.; Xie, Y.L.; Mwanza, A.D.; Li, T.-H. Research on Freeze-thaw Cycle Expansion of Coarse Grained Acid Salt Saline Soil. *J. Zhengzhou Univ. (Eng. Sci.)* **2011**, *32*, 75–79.
18. Bao, W.X.; Li, Z.N. Testing on transmutation properties of saline soil under freezing and thawing cycles in Kashi, Xinjiang. *J. Chang. Univ. Nat. Sci. Ed.* **2008**, *2*, 26–30. (In Chinese)
19. Li, Y.; Zhang, Y.F.; Shi, Q.; Lu, H.T.; Liu, K. Experimental Research on Freezing-thawing Cycles of Crude Saline Soil in Lop Nur Area. *J. Sci. Technol. Eng.* **2015**, *15*, 194–197. (In Chinese)
20. Hu, H. Experimental study on frost heave of natural sulfite soil salt in Lop Nur. *J. Water Resour. Hydropower Northeast. China* **2021**, *39*, 39–40. (In Chinese)
21. Pan, L.; Zhang, Y.F.; Cheng, J.Z.; Zhang, Y.H. Research on salt -frost expansion rules of sulfurous saline soil during each freeze -thaw cycle. *J. Water Resour. Water Eng.* **2018**, *29*, 220–224. (In Chinese)
22. Na, S.S. Research on salt-frost heave test of natural sulphate saline soil. *J. Shanxi Archit.* **2015**, *41*, 69–70. (In Chinese)
23. Liu, Y.W.; Wang, Q.; Liu, S.W.; ShangGuan, Y.; Fu, H.; Ma, B.; Chen, H.; Yuan, X. Experimental investigation of the geotechnical properties and microstructure of lime-stabilized saline soils under freeze-thaw cycling. *J. Cold Reg. Sci. Technol.* **2019**, *161*, 32–42. [[CrossRef](#)]
24. Han, Z.Q.; Bao, W.X. Expansion Characteristics and Microstructure Mechanism of Salt Saline Subgrade with Freezing and Thawing Cycles. *J. Transp. Res.* **2011**, *14*, 96–99. (In Chinese)
25. Wang, J.; Wang, Q.; Lin, S.; Han, Y.; Cheng, S.; Wang, N. Relationship between the shear strength and microscopic pore parameters of saline soil with different freeze-thaw cycles and salinities. *Symmetry* **2020**, *12*, 1709. [[CrossRef](#)]
26. Zhang, S.S.; Xie, Y.L.; Yang, X.H.; Dai, Z.R. Research on microstructure of crude coarse grain saline soil under freezing and thawing cycles. *J. Rock Soil Mech.* **2010**, *31*, 123–127. (In Chinese)
27. Bao, W.X.; Yang, X.H.; Xie, Y.L. Research on salt expansion of representative crude saline soil under freezing and thawing cycles. *J. Geotech. Eng.* **2006**, *28*, 1991–1995. (In Chinese)
28. Chamberlain, E.J.; Gow, A.J. Effect of freezing and thawing on the permeability and structure of soils. *Eng. Geol.* **1979**, *13*, 73–92. [[CrossRef](#)]
29. Xiao, Z.; Lai, Y.; Zhang, M. Study on the freezing temperature of saline soil. *J. Acta Geotech.* **2018**, *13*, 195–205. [[CrossRef](#)]
30. Bing, H.; Ma, W. Laboratory investigation of the freezing point of saline soil. *J. Cold Reg. Sci. Technol.* **2011**, *67*, 79–88. [[CrossRef](#)]
31. Wan, X.; Yang, Z.J. Pore water freezing characteristic in saline soils based on pore size distribution. *J. Cold Reg. Sci. Technol.* **2020**, *173*, 103030. [[CrossRef](#)]
32. Zhang, J.; Lai, Y.; Li, J.; Zhao, Y. Study on the influence of hydro-thermal-salt-mechanical interaction in saturated frozen sulfate saline soil based on crystallization kinetics. *Int. J. Heat Mass Transf.* **2020**, *146*, 118868. [[CrossRef](#)]
33. Wan, X.S.; Liao, M.K.; Du, L.Q. Experimental Study on the Influence of Temperature on Salt Expansion of Sodium Sulfate Saline Soil. *J. Highw. Transp. Res. Dev.* **2017**, *11*, 1–7. [[CrossRef](#)]
34. Wang, J.C.; Li, J.S.; Wang, C.M. A Study on Single-cycle Salt and Frost Heaving of Sulfate (Sulfurous) Saline Soil. *J. Jilin Univ.* **2006**, *36*, 410–416. [[CrossRef](#)]
35. Wen, T.; Ying, S.; Zhou, F. Calculation of salt-frost heave of sulfate saline soil due to long-term freeze-thaw cycles. *J. Cold Arid Reg.* **2020**, *12*, 284–294. [[CrossRef](#)]
36. Younes, A. On modelling the multidimensional coupled fluid flow and heat or mass transport in porous media. *J. Int. J. Heat Mass Transf.* **2003**, *46*, 367–379. [[CrossRef](#)]
37. Nguyen, T.Q.; Petkovi, J.; Dangla, P.; Baroghel-Bouny, V. Modelling of coupled ion and moisture transport in porous building materials. *J. Constr. Build. Mater.* **2008**, *22*, 2185–2195. [[CrossRef](#)]
38. Koniorczyk, M.; Gawin, D. Heat and Moisture Transport in Porous Building Materials Containing Salt. *J. Build. Phys.* **2008**, *31*, 279–300. [[CrossRef](#)]

39. Zhang, X.; Wang, Q.; Wang, G.; Wang, W.; Chen, H.; Zhang, Z. A Study on the Coupled Model of Hydrothermal-Salt for Saturated Freezing Salinized Soil. *J. Math. Probl. Eng.* **2017**, *2017*, 4918461. [[CrossRef](#)]
40. Zhang, X.; Wang, Q.; Yu, T.; Wang, G.; Wang, W. Numerical Study on the Multifield Mathematical Coupled Model of Hydraulic-Thermal-Salt-Mechanical in Saturated Freezing Saline Soil. *Int. J. Geomech.* **2018**, *18*, 04018064. [[CrossRef](#)]
41. Ren, X.L.; Zhang, W.; Liu, X. The Research Development and Thinking About the Expansibility Property of Saline Soil in Northwest Region. *Chin. J. Soil Sci.* **2016**, *47*, 246–252. (In Chinese)
42. Wu, Y.P.; Liang, H.; Wei, M.Q. Influence of Gradation on Subsidence Characteristic of Coarse Particle Sulphate Soil. *J. Railw. Eng. Soc.* **2019**, *36*, 12–16.
43. Liu, X.Z.; Wu, Y.; Pan, S.T.; Liu, X.; Gu, M. Influences of different grain size contents on soil-water characteristic curve of unsaturated laterite based on fractal theory. *J. Hydro-Sci. Eng.* **2018**, *5*, 103–110. (In Chinese)
44. Cheng, Y.L.; Uchimura, T. Influence of particle size on water retention of soils. *Chin. J. Rock Mech. Eng.* **2016**, *35*, 1474–1482. (In Chinese)